A&A 445, 29–42 (2006)
DOI: 10.1051/0004-6361:20052954

Astronomy & Astrophysics

RASS-SDSS Galaxy cluster survey

IV. A ubiquitous dwarf galaxy population in clusters

P. Popesso[1], A. Biviano[2], H. Böhringer[1], and M. Romaniello[3]

[1] Max-Planck-Institut fur extraterrestrische Physik, 85748 Garching, Germany
e-mail: ppopesso@eso.org
[2] INAF – Osservatorio Astronomico di Trieste, via G. B. Tiepolo 11, 34131, Trieste, Italy
[3] European Southern Observatory, Karl Scharzschild Strasse 2, 85748, Germany

Received 1 March 2005 / Accepted 8 June 2005

ABSTRACT

We analyze the Luminosity Functions (LFs) of a subsample of 69 clusters from the RASS-SDSS galaxy cluster catalog. When calculated within the cluster physical sizes, given by r_{200} or r_{500}, all the cluster LFs appear to have the same shape, well fitted by a composite of two Schechter functions with a marked upturn and a steepening at the faint-end. Previously reported cluster-to-cluster variations of the LF faint-end slope are due to the use of a metric cluster aperture for computing the LF of clusters of different masses.
We determine the composite LF for early- and late-type galaxies, where the typing is based on the galaxy $u - r$ colors. The late-type LF is well fitted by a single Schechter function with a steep slope ($\alpha = -2.0$ in the r band, within r_{200}). The early-type LF instead cannot be fitted by a single Schechter function, and a composite of two Schechter functions is needed. The faint-end upturn of the global cluster LF is due to the early-type cluster galaxies. The shape of the bright-end tail of the early-type LF does not seem to depend upon the local galaxy density or the distance from the cluster center. The late-type LF shows a significant variation only very near the cluster center. On the other hand, the faint-end tail of the early-type LF shows a significant and continuous variation with the environment.
We provide evidence that the process responsible for creating the excess population of dwarf early type galaxies in clusters is a threshold process that occurs when the density exceeds ∼500 times the critical density of the Universe.
We interpret our results in the context of the "harassment" scenario, where faint early-type cluster galaxies are predicted to be the descendants of tidally-stripped late-type galaxies.

Key words. galaxies: clusters: general – galaxies: luminosity function, mass function

1. Introduction

The galaxy Luminosity Function (LF) is a fundamental tool for understanding galaxy evolution and faint galaxy populations. The shape of the cluster LF provides information on the initial formation and subsequent evolution of galaxies in clusters while the slope of the faint-end indicates how steeply the dwarf number counts rise as a function of magnitude.

Much work has been done on the cluster LF, with various groups finding differences in its shape and the faint-end slope. Different techniques have been used to measure LFs of individual clusters or to make a composite LF from individual clusters LFs (e.g. Dressler 1978; Lugger 1986, 1989; Colless 1989; Biviano et al. 1995; Lumsden et al. 1997; Valotto et al. 1997; Rauzy et al. 1998; Garilli et al. 1999; Paolillo et al. 2001; Goto et al. 2002; Yagi et al. 2002; Popesso et al. 2004a). Whether the LF of cluster galaxies is universal or not, and whether it is different from the LF of field galaxies are still debated issues. Several authors (Dressler 1978; Lumdsen et al. 1997; Valotto et al. 1997; Garilli et al. 1999; Goto et al. 2002; Christlein & Zabludoff 2003) have found significant differences between the LFs of different clusters as well as between the LFs of cluster and field galaxies, while others (Lugger 1986, 1989; Colless 1989; Rauzy et al. 1998; Trentham 1998; Paolillo et al. 2001; Andreon 2004) have concluded that the galaxy LF is universal in all environments. Another debated issue is the slope of the faint end of the LF of cluster galaxies (see, e.g., Driver et al. 1994; De Propris et al. 1995; Lobo et al. 1997; Smith et al. 1997; Phillipps et al. 1998; Boyce et al. 2001; Beijersbergen et al. 2001; Trentham et al. 2001; Sabatini et al. 2003; Cortese et al. 2003). The LF of cluster galaxies is typically observed to steepen faint-ward of $M_g \sim -18$, with power-law slopes $\alpha \sim -1.8 \pm 0.4$. This corresponds to the debated upturn of the cluster LF due to an excess of dwarf galaxies relative to the field LF. The effect may be real, and due to cluster environmental effects, but it could also be generated by systematics in the detection techniques of faint, low surface-brightness galaxies.

In Popesso et al. (2004a, hereafter Paper II) we have recently analyzed the LF of clusters from the RASS-SDSS

(ROSAT All Sky Survey – Sloan Digital Sky Survey) galaxy clusters survey down to −14 mag. We concluded that the composite cluster LF is characterized by an upturn and a clear steepening at faint magnitudes, in all SDSS photometric bands. Different methods of background subtraction were shown to lead to the same LF. The observed upturn of the LF at faint magnitudes was shown in particular not to be due to background contamination by large scale structures or multiple clusters along the same line of sight. We concluded that the observed steepening of the cluster LF is due to the presence of a real population of faint cluster galaxies.

The composite LF was well fitted by the sum of two Schechter (1976) functions. The LF at its bright-end was shown to be characterized by the classical slope of −1.25 in all photometric bands, and a decreasing M^* from the z to the g band. The LF at its faint-end was found to be much steeper than the LF at its bright-end, and characterized by a power-law slope $-2.5 \leq \alpha \leq -1.6$. The observed upturn of the LF was found to occur at −16 in the g band, and at −18.5 in the z band.

A steep mass function of galactic halos is a robust prediction of currently popular hierarchical clustering theories for the formation and evolution of cosmic structure (e.g. Kauffmann et al. 1993; Cole et al. 1994). This prediction conflicts with the flat galaxy LF measured in the field and in local groups, but is in agreement with the steep LF measured in the RASS-SDSS clusters. Two models have been proposed to explain the observed environmental dependence of the LF. According to Menci et al. (2002), merging processes are responsible for the flattening of the LF; the environmental dependence arises because mergers are more common in the field (or group) environment than in clusters, where they are inhibited by the high velocity dispersion of galaxies. According to Tully et al. (2002), instead, the LF flattening is due to inhibited star formation in dark matter halos that form late, i.e. after photoionization of the intergalactic medium has taken place. Since dark matter halos form earlier in higher density environments, a dependence of the observed LF slope on the environment is predicted. On the other hand, if reionization happens very early in the Universe, this scenario may not work (Davies et al. 2005). Other physical processes are however at work in the cluster environment, such as ram-pressure stripping (Gunn & Gott 1972) and galaxy harassment (e.g. Moore et al. 1996, 1998), which are able to fade cluster galaxies, particularly the less massive ones. Whether the outcome of these processes should be a steepening or a flattening of the LF faint-end is still unclear.

In Paper II it was also shown that the bright-end of the LF is independent from the cluster environment, and the same in all clusters. On the other hand, the LF faint-end was found to vary from cluster to cluster. In the present paper (IV in the series of the RASS-SDSS galaxy cluster survey) we show that the previously found variations of the faint end of the cluster LF are due to aperture effects. In other words, when measured within the physical size of the system, given by either r_{200} or r_{500}, the LF is invariant for all clusters, both at the bright and at the faint end. We also analyze how the number ratio of dwarf to giant galaxies in galaxy clusters depends on global cluster properties such as the velocity dispersion, the mass, and the X-ray and optical luminosities. Finally, we investigate the nature of the dwarf galaxies in clusters by studying their color distribution and suggest a possible formation scenario for this population.

The paper is organized as follows. In Sect. 2 of the paper we describe our dataset. In Sect. 3 we summarize the methods used to calculate the individual and the composite cluster LFs. In Sect. 4 we summarize our methods for measuring the clusters characteristic radii. In Sect. 5 we analyze the resulting composite and individual LFs. In Sect. 6 we determine the cluster composite LF per galaxy type. In Sect. 7 we analyse the environmental dependence of the LF, and compare the cluster and field LFs. In Sect. 8 we provide our discussion, suggesting a possible formation scenario for the faint galaxy population in clusters. Finally, in Sect. 9 we draw our conclusions.

For consistency with Paper II and with previous works, we use $H_0 = 100\ h$ km s^{-1} Mpc^{-1}, $\Omega_{\rm m} = 0.3$ and $\Omega_\Lambda = 0.7$ throughout the paper.

2. The data

In order to study the variation of the cluster LF from system to system, the analysis has to be applied to a large statistical sample of clusters, covering the whole spectrum of properties (in mass, richness, X-ray luminosity and optical luminosity) of the systems considered. Since the X-ray observations provide a robust method of identification of galaxy clusters and the X-ray luminosity is a good estimator of the system total mass and optical luminosity (see Paper I; and Popesso et al. 2004c, hereafter Paper III), we have used for our purpose the RASS-SDSS galaxy cluster sample, which is an X-ray selected sample of objects in a wide range of X-ray luminosity. The updated version of the RASS-SDSS galaxy cluster catalog comprises 130 systems detected in the RASS and in the SDSS sky region (16 clusters more than in the first version of the catalog released in Paper I due to the larger sky area available in the SDSS DR2). The X-ray cluster properties and the cluster redshifts have been taken from a variety of X-ray catalogs, that allow to cover the whole L_X spectrum. The X-ray intermediate and bright clusters have been selected from three ROSAT based cluster samples: the ROSAT-ESO flux limited X-ray cluster sample (REFLEX, Böhringer et al. 2002), the Northern ROSAT All-sky cluster sample (NORAS, Böhringer et al. 2000), the NORAS 2 cluster sample (Retzlaff 2001). The X-ray faint clusters and the groups have been selected from two catalogs of X-ray detected objects: the ASCA Cluster Catalog (ACC) from Horner (2001) and the Group Sample (GS) of Mulchaey et al. (2003). The RASS-SDSS galaxy cluster sample comprises only nearby systems at the mean redshift of 0.1. The sample covers the entire range of masses and X-ray luminosities, from very low-mass and X-ray faint groups ($10^{13}\ M_\odot$ and 10^{42} erg s^{-1}) to very massive and X-ray bright clusters ($5\times10^{15}\ M_\odot$ and 5×10^{44} erg s^{-1}).

The optical photometric data are taken from the 2nd data release of the SDSS (Fukugita et al. 1996; Gunn et al. 1998; Lupton et al. 1999; York et al. 2000; Hogg et al. 2001; Eisenstein et al. 2001; Smith et al. 2002; Strauss et al. 2002; Stoughton et al. 2002; Blanton et al. 2003; and Abazajian et al. 2003). The SDSS consists of an imaging survey of π steradians of the northern sky in the five passbands u, g, r, i, z,. The imaging data are processed with a photometric pipeline (PHOTO)

specially written for the SDSS data. For each cluster we defined a photometric galaxy catalog as described in Sect. 3 of Popesso et al. (2004b, Paper I). For the analysis in this paper we only use SDSS Model magnitudes (see Paper II for details).

In this paper we consider a subsample of 69 clusters of the RASS-SDSS sample for which the masses, velocity dispersion, r_{200} and r_{500} (see Sect. 4) were derived through the virial analysis (see Paper III) applied to the spectroscopic galaxy members of each systems.

Since throughout the paper the results obtained with the current analysis of the cluster LF are often compared with the results obtained in Paper II, it is important to notice that the cluster sample used here is a subsample of the dataset used in Paper II.

3. Determination of the individual and composite Luminosity Functions

We here summarize the methods by which we measure the individual and composite cluster LFs. Full details can be found in Papers I and II.

We consider two different approaches to the statistical subtraction of the galaxy background. As a first approach, we calculate a local background in an annulus centered on the X-ray cluster center with an inner radius of 3 h^{-1} Mpc and a width of 0.5 deg.

As a second approach we derive a global background correction. We define as $N^{\rm g}_{\rm bg}(m){\rm d}m$ the mean of the galaxy number counts determined in five different SDSS sky regions, randomly chosen, each with an area of 30 deg^2. A detailed comparison of the local and global background estimates can be found in Paper I. The results shown in this paper are obtained using a global background subtraction.

We derive the LFs of each cluster by subtracting from the galaxy counts measured in the cluster region, the field counts rescaled to the cluster area. Following previous literature suggestions, we exclude the brightest cluster galaxies from the clusters LFs.

In order to convert from apparent to absolute magnitudes we use the cluster luminosity distance, correct the magnitudes for the Galactic extinction (obtained from the maps of Schlegel et al. 1998), and apply the K-correction of Fukugita et al. (1995) for elliptical galaxies, which are likely to constitute the main cluster galaxy population.

The composite LF is obtained following Colless (1989) prescriptions. A detailed description of the method can be found in Paper II.

3.1. Low surface brightness selection effect

It is well known that magnitude-limited surveys may be biased against low-surface brightness galaxies (e.g. Phillips & Driver 1995). An assessment of this bias for the SDSS-EDR and SDSS-DR1 has been done by Cross et al. (2004), who compared these catalogs with the Millennium Galaxy Catalog (Liske et al. 2003), a deep survey limited in surface brightness to 26 mag arcsec^{-2}. Cross et al. (2004) concluded that the incompleteness of SDSS-EDR is less than 5% in the range of effective surface-brightness $21 \leq \mu_{\rm e} \leq 25$ mag arcsec^{-2}, and it is around 10% in the range $25 \leq \mu_{\rm e} \leq 26$ mag arcsec^{-2}. In this paper, galaxies contributing to the faint-end of the cluster LFs have magnitudes $18 \leq r \leq 21$. In this magnitude range, 65% of the objects have $\mu_{\rm e} \leq 23$ mag arcsec^{-2}, 30% have $23 < \mu_{\rm e} \leq 24$ mag arcsec^{-2}, and 5% have $mu_{\rm e} \geq 25$ mag arcsec^{-2}. Hence, from the results of Cross et al. (2004), we do not expect that the bias against low surface-brightness galaxies results in an incompleteness above ∼5%. The faint-end of the cluster LFs derived in this paper should thus be quite unaffected by this selection effect.

4. The characteristic radii of galaxy clusters

We here describe the methods by which we measure the characteristic radii r_{500} and r_{200}. r_{200} is the radius where the mass density of the system is 200 times the critical density of the Universe and it is considered as a robust measure of the virial radius of the cluster. Similarly, r_{500} is defined setting 500 instead of 200 in the previous definition and it samples the central region of the cluster. Full details can be found in Paper III.

We estimate a cluster characteristic radius through the virial analysis applied on the redshifts of its member galaxies. We use the redshifts provided in the SDSS spectroscopic catalog to define the galaxy membership of each considered system. The SDSS spectroscopic sample comprises all the objects observed in the Sloan r band with pretrosian magnitude $r_{\rm P} \leq 17.77$ mag and half-light surface brightness $\mu_{50} \leq 24.5$ mag arcsec^{-2}. The SDSS DR2 spectrocsopic sample used for this analysis counts more tha 250 000 galaxies.

Cluster members are selected following the method of Girardi et al. (1993). First, among the galaxies contained in a circle of radius equal to the Abell radius, those with redshift $|cz - cz_{\rm cluster}| > 4000$ km s^{-1} are removed, where $z_{\rm cluster}$ is the mean cluster redshift. Then, the gapper procedure (see also Beers et al. 1990) is used to define the cluster limits in velocity space. Galaxies outside these limits are removed. Finally, on the remaining galaxies we apply the interloper-removal method of Katgert et al. (2004; see Appendix A in that paper for more details).

The virial analysis (see, e.g., Girardi et al. 1998) is then performed on the clusters with at least 10 member galaxies. The velocity dispersion is computed using the biweight estimator (Beers et al. 1990). The virial masses are corrected for the surface-pressure term (The & White 1986), using a Navarro et al. (1996, 1997) mass density profile, with concentration parameter $c = 4$. This profile provides a good fit to the observationally determined average mass profile of rich clusters (see Katgert et al. 2004).

Our clusters span a wide range in mass; since clusters of different masses have different concentrations (see, e.g. Dolag et al. 2004) we should in principle compute the cluster masses, M's, using a different concentration parameter c for each cluster. According to Dolag et al. (2004), $c \propto M^{-0.102}$. Taking $c = 4$ for clusters as massive as those analysed by Katgert et al. (2004), $M \simeq 2 \times 10^{15}\ M_{\odot}$, Dolag et al.'s scaling implies our clusters span a range $c \simeq 3$–6. Using $c = 6$ instead of $c = 4$ makes the mass estimates 4% and 10% higher at, respectively,

r_{200} and r_{500}, while using $c = 3$ makes the mass estimates lower by the same factors. This effect being clearly much smaller than the observational uncertainties, we assume the same $c = 4$ in the analysis for all clusters.

If $M_{\rm vir}$ is the virial mass (corrected for the surface-pressure term) contained in a volume of radius equal to the clustercentric distance of the most distant cluster member in the sample, i.e. the aperture radius $r_{\rm ap}$, then, the radius r_{200} is then given by:

$$r_{200} \equiv r_{\rm ap}\,[\rho_{\rm vir}/(200\rho_{\rm c})]^{1/2.4} \quad (1)$$

where $\rho_{\rm vir} \equiv 3M_{\rm vir}/(4\pi r_{\rm ap}^3)$ and $\rho_{\rm c}(z)$ is the critical density at redshift z in the adopted cosmology. The exponent in Eq. (1) is the one that describes the average cluster mass density profile near r_{200}, as estimated by Katgert et al. (2004) for an ensemble of 59 rich clusters. Similarly, r_{500} is estimated by setting 500 instead of 200 in Eq. (1).

5. Analysis of the individual and composite LFs

In order to analyze the behavior of the composite LF faint-end as a function of waveband and clustercentric distance, we define the number ratio of dwarf to giant galaxies, DGR, as the ratio between the number of faint ($-18 \leq M \leq -16.5$) and bright ($M < -20$) galaxies in the cluster LF. The DGR is found to vary from cluster to cluster, more than expected from statistical errors. These variations are not random however. As shown in Fig. 1, when the DGRs are computed within a fixed metric radius, they are significantly anti-correlated with several cluster global properties, i.e. the cluster velocity dispersions, masses, and X-ray and optical luminosities (velocity dispersions, virial masses, and X-ray luminosities for our cluster sample were derived in Paper III). All the correlations are very significant (1–5×10^{-5}, according to a Spearman correlation test). The more massive a cluster, the lower its fraction of dwarf galaxies.

The correlation between cluster DGRs and cluster masses is most likely due to the choice of a fixed metric aperture for all the clusters. In fact, a fixed metric aperture samples larger (smaller) fractions of the virialized regions of clusters of smaller (respectively, larger) masses, and DGR is known to increase with clustercentric distance (Paper II).

Because of this effect, the different cluster physical sizes must be taken into account before comparing different cluster LFs. We then determine the individual and composite LFs within r_{500} and r_{200} for the subsample of 69 clusters of the RASS-SDSS galaxy cluster sample for which these parameters are known (see Paper III).

The composite LF calculated within r_{200} is shown in Fig. 2 for four SDSS photometric bands. The u-band LF is not shown; in this band, there is no evidence for an upturn at faint magnitude levels (see Paper II). For all the other bands LFs, a single Schechter function does not provide acceptable fits, and a composite of two Schechter functions is needed:

$$\phi(L) = \phi^* \left[\left(\frac{L}{L^*_{\rm b}}\right)^{\alpha_b} \exp\left(\frac{-L}{L^*_{\rm b}}\right) + \left(\frac{L^*_{\rm b}}{L^*_{\rm f}}\right) \times \left(\frac{L}{L^*_{\rm f}}\right)^{\alpha_{\rm f}} \exp\left(\frac{-L}{L^*_{\rm f}}\right)\right] \quad (2)$$

where b and f label the Schechter parameters of the bright and faint end respectively. From the reduced-χ^2 values given in Table 1 we conclude that a double-Schechter function does provide adequate fits to the 4-bands composite LFs. Alternatively, we fit the composite LFs with a function of this form:

$$\phi(L) = \phi^* \left(\frac{L}{L^*}\right)^{\alpha} \exp\left(\frac{-L}{L^*}\right)\left[1 + \left(\frac{L}{L_{\rm t}}\right)^{\beta}\right]. \quad (3)$$

In this function, ϕ^*, L^* and α are the standard Schechter parameters, $L_{\rm t}$ is a transition luminosity between the two power laws and β is the power law slope of the very faint end (Loveday 1997). Both functions require the same number of fit parameters. However, the double Schechter component function provides slightly better fits than the Schechter+power-law function in all the Sloan bands (see Table 1).

The Double Schechter function has been used for the first time by Driver et al. (1994), while Thompson & Gregory (1993) and Biviano et al. (1995) suggested a Gaussian+Schechter function, to fit respectively the bright and the faint end of the LF. More recently, Hilker et al. (2003) used a double Schechter Function to fit the LF of the Fornax cluster.

The confidence-level contours of the best-fit parameters of the bright- and faint-end Schechter components are shown in Figs. 3 and 4, respectively. Both results for the composite LF within r_{500} (dotted contours) and r_{200} (solid contours) are shown. Clearly, the best-fit Schechter function to the LF bright-end does not change significantly from r_{500} to r_{200} (see Fig. 3) confirming the findings of Paper II. However, the faint-end LF steepens significantly (by 0.1–0.15 dex) from r_{500} to r_{200}, and the characteristic magnitude correspondingly brightens by 0.3–0.4 magnitudes (see Fig. 4), thereby indicating an increasing DGR with radius. Our result is in agreement with the findings of Paper II, and several other works in the literature, which were however mostly based on single cluster studies (e.g. Lobo et al. 1997; Durret et al. 2002; Mercurio et al. 2003; Pracy et al. 2004; see however Trentham et al. 2001, for a discordant result).

While our conclusions on the composite LF agree with those of Paper II, we find here different results concerning the individual cluster LFs. While in Paper II we claimed significant LF variations from cluster to cluster, we discover that such variations disappear when the individual cluster LFs are computed within the physical sizes of each cluster (defined by r_{500} or r_{200}). This can be seen in Fig. 5a, where we plot the individual LFs of 15 clusters (those with the faintest absolute magnitude limits) and, superposed, the composite LF, all measured within r_{200} and in the r-band. The agreement between the composite and individual LFs is very good. Fitting the composite LF to the individual cluster LFs result in the reduced-χ^2 distribution shown in Fig. 5b. For 90% of the clusters the probability that the composite and individual LFs are drawn from the same parent distribution is larger than 95%.

In Fig. 5c we also show the z-band DGR-distribution. When compared to the DGR distribution found in Paper II, the new DGR distribution is much narrower. In this paper we considered the DGR within r_{200} of 29 clusters, those with known mass, r_{200} and r_{500}, out of the 35 systems considered in Paper II. The mean value of the DGR is 3.5 and its dispersion is indeed very close to the mean DGR statistical error of 1.4, as expected

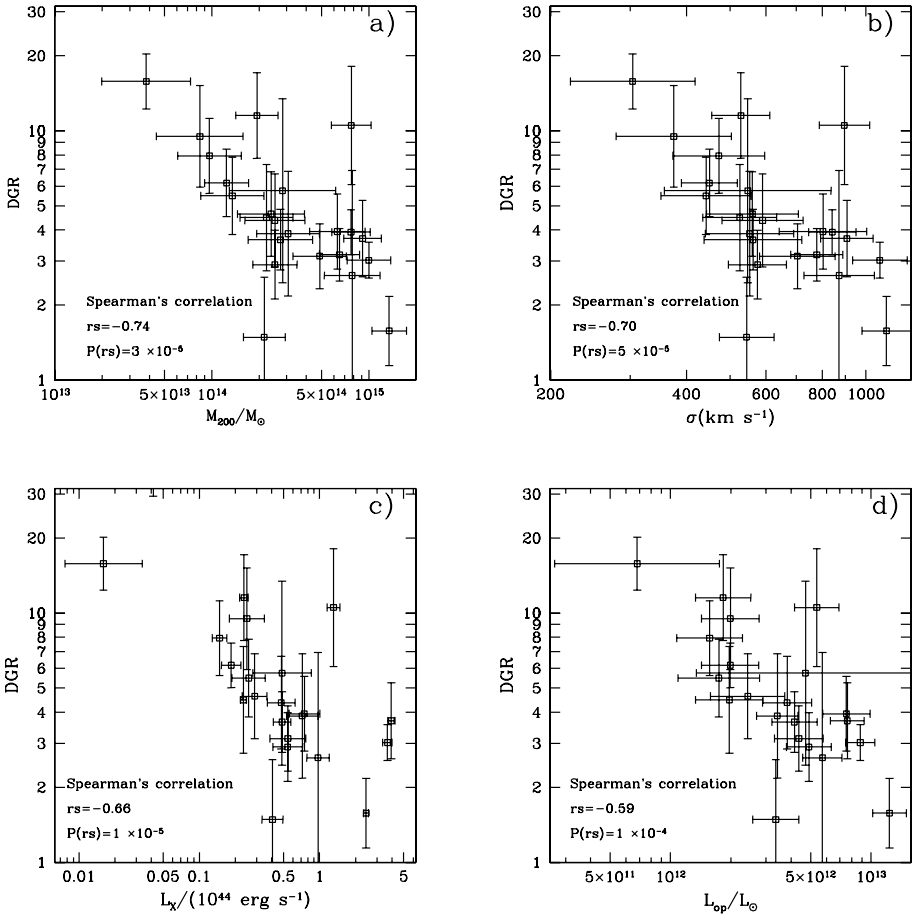

Fig. 1. The z-band DGR vs. the cluster mass (panel **a)**), the velocity dispersion σ (panel **b)**), the X-ray luminosity (panel **c)**), and the optical luminosity (panel **d)**). The DGR is calculated within a circle of 1 Mpc radius centered on the X-ray cluster center. In each panel, we list the value of the Spearman's rank correlation coefficient and the implied probability of no correlation.

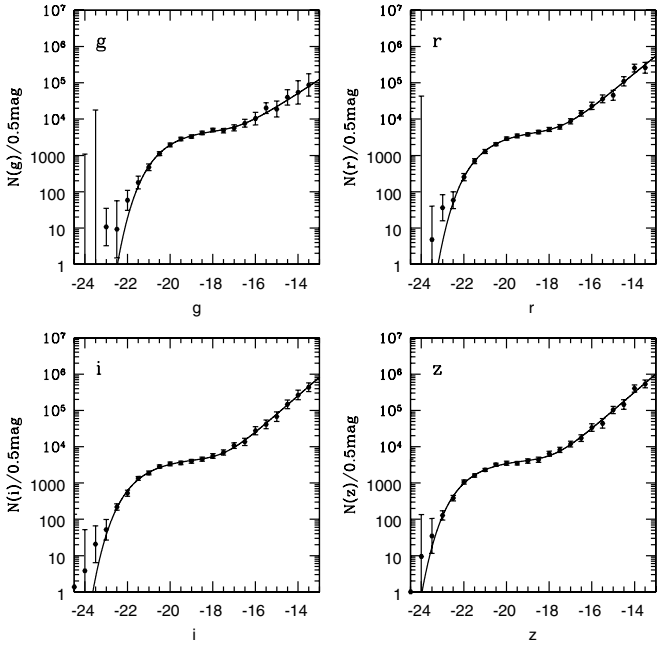

Fig. 2. The 4 panels show the composite LFs in the 4 Sloan bands. The individual LFs used to calculate the composite LFs are measured within the physical sizes of the clusters, as given by r_{200}.

if the individual cluster LFs are indeed all rather similar when computed within a cluster-related physical radius.

Finally, in Fig. 6 we show DGR within r_{200} as a function of the cluster mass M_{200} (panel a) and the velocity dispersion (panel b). There is no hint of the relation previously found (compare with Fig. 1a): the Spearman correlation coefficient is −0.08, which is not statistically significant. Similar results are found also for the $DGR - L_X$ and $DGR - L_{op}$ relations.

Hence we conclude that the cluster to cluster LF variation seen in Paper II are entirely due to the use of a fixed metric aperture for all clusters, rather than an aperture sampling the same fraction of the virialized region of each cluster.

6. The cluster LF per galaxy type

In order to better understand the nature of the cluster galaxies responsible for the LF upturn at low luminosities, we examine their color distribution. In particular, we use the $u - r$ color, since the $u - r$ distribution of Sa and earlier-type galaxies is well separated from the $u - r$ distribution of Sb and later-type galaxies (Strateva et al. 2001), thereby allowing to distinguish the two morphological samples down to very faint magnitudes.

To define the color distribution of the cluster galaxies we statistically subtract the contribution of field galaxies

Table 1. Schechter parameters of the composite LF.

	g	r	i	z
Double Schechter components function within r_{200}				
α_b	-1.07 ± 0.12	-1.09 ± 0.09	-1.08 ± 0.08	-1.07 ± 0.08
M^*_b	-20.18 ± 0.21	-20.94 ± 0.16	-21.35 ± 0.16	-21.69 ± 0.15
α_f	-1.98 ± 0.16	-2.19 ± 0.09	-2.26 ± 0.07	-2.25 ± 0.07
M^*_f	-17.37 ± 0.21	-18.14 ± 0.15	-18.43 ± 0.15	-18.66 ± 0.14
χ^2/ν	0.89	1.05	1.15	1.16
Double Schechter components function within r_{500}				
α_b	-0.97 ± 0.09	-1.05 ± 0.07	-1.06 ± 0.06	-1.05 ± 0.05
M^*_b	-20.04 ± 0.15	-20.84 ± 0.13	-21.36 ± 0.14	-21.67 ± 0.13
α_f	-1.84 ± 0.11	-2.02 ± 0.06	-2.17 ± 0.05	-2.19 ± 0.06
M^*_f	-16.61 ± 0.22	-17.38 ± 0.13	-17.49 ± 0.12	-17.58 ± 0.12
χ^2/ν	0.87	0.98	1.11	1.09
Schechter+exponential function within r_{200}				
α	-0.88 ± 0.25	-1.26 ± 0.12	-1.16 ± 0.13	-1.16 ± 0.12
M^*	-19.95 ± 0.29	-21.16 ± 0.26	-21.41 ± 0.22	-21.71 ± 0.20
β	-1.40 ± 0.05	-1.30 ± 0.07	-1.26 ± 0.08	-1.25 ± 0.07
M^*_t	-17.27 ± 0.22	-16.99 ± 0.43	-17.65 ± 0.41	-17.80 ± 0.39
χ^2/ν	1.10	1.15	1.38	1.40
Schechter+exponential function within r_{500}				
α	-0.88 ± 0.25	-1.05 ± 0.16	-1.22 ± 0.14	-1.00 ± 0.14
M^*	-19.94 ± 0.29	-20.91 ± 0.28	-21.40 ± 0.25	-21.54 ± 0.21
β	-1.33 ± 0.14	-1.33 ± 0.09	-1.22 ± 0.06	-1.28 ± 0.08
M^*_t	-16.95 ± 0.63	-17.28 ± 0.50	-17.43 ± 0.52	-17.93 ± 0.45
χ^2/ν	1.13	1.15	1.41	1.43

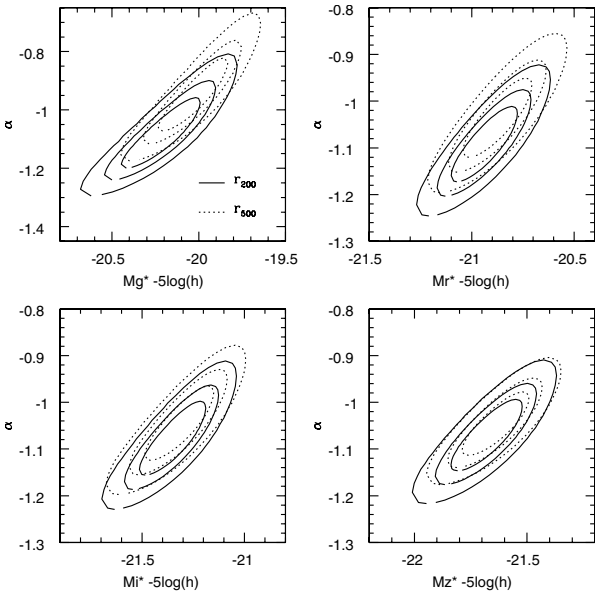

Fig. 3. Contour plots of the 68%, 95%, and 99% confidence levels of the parameters of the bright-end component of the double-Schechter function fit to the 4 SDSS bands composite LFs. Solid (dotted) contours show the results for the composite LF computed within r_{200} (respectively r_{500}).

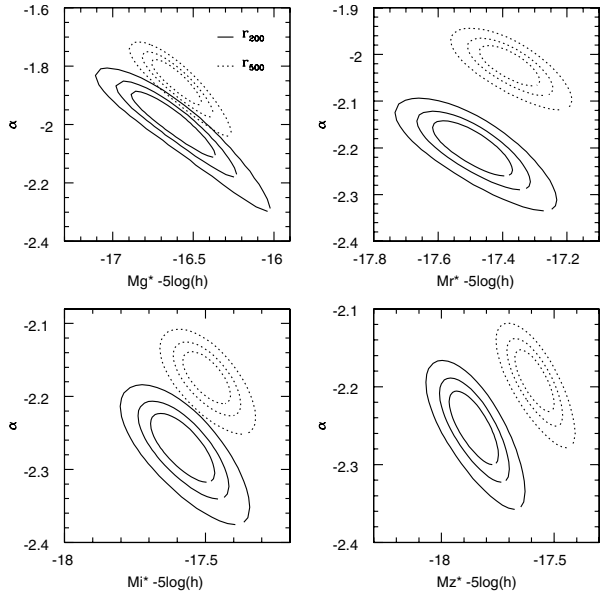

Fig. 4. Same as Fig. 3, but for the faint-end component.

(Boyce et al. 2001), using the same method applied for the statistical subtraction of the background from the magnitude number counts. We determine the background color distribution of field galaxies in an annulus around the cluster with inner radius larger than r_{200}; significantly under- or over-dense regions (e.g. voids and background clusters) are excluded. By subtracting the background color distribution from the color distribution of galaxies in the cluster region, we obtain the $u-r$ distribution of cluster galaxies. The validity of the method is confirmed by its application to the spectroscopic subsample, for which cluster membership can be established from the galaxy redshifts.

Figure 7 shows the (background-subtracted) $u-r$ distribution of cluster galaxies in the range $-18 \leq r \leq -16.5$ (panel a) and $-16.5 \leq r \leq -15$ (panel b) for the subsample of 15 clusters with the faintest absolute magnitude limit in the r band

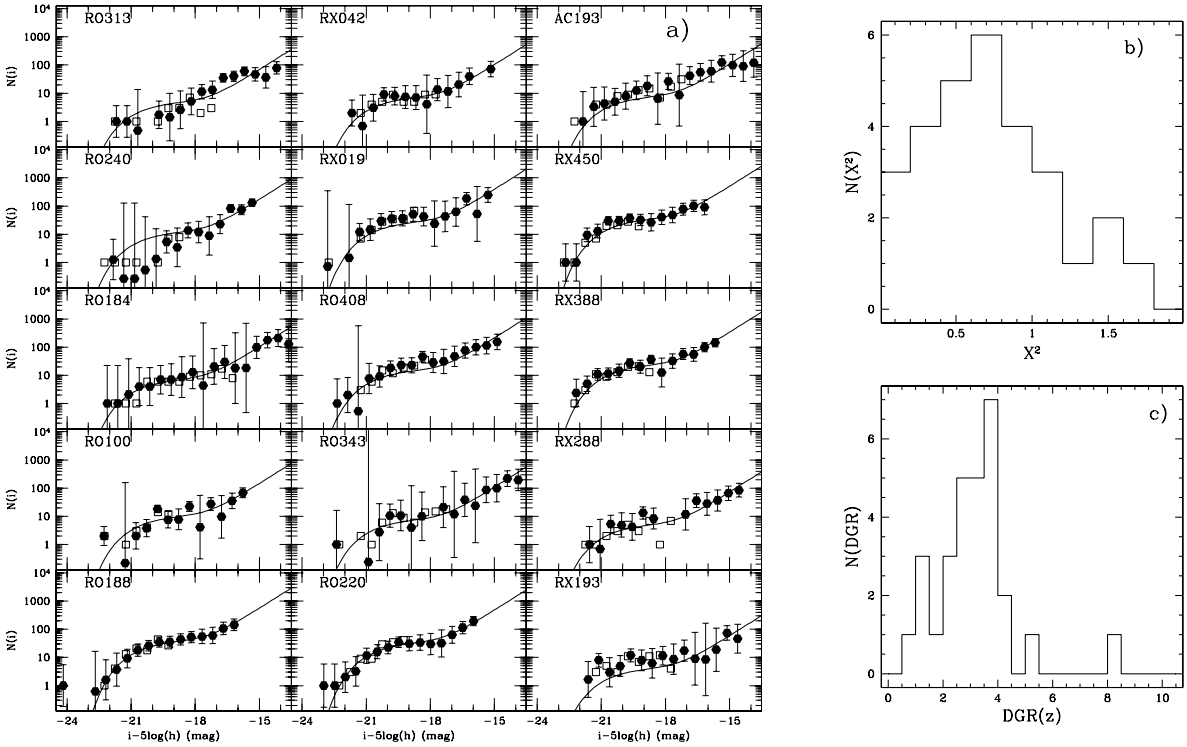

Fig. 5. Panel **a)**: the individual r-band LFs within r_{200} of a subsample of 15 clusters with the faintest absolute magnitude limit ($M_{r,\rm lim} \leq -15.5$). Empty squares and filled points distinguish the LFs computed from cluster members only (down to the SDSS spectroscopic completeness magnitude, $r \leq 17.77$), and using a statistical background subtraction, respectively. The solid line is the composite LF. Cluster names are indicated. Panel **b)**: the distribution of the χ^2 values obtained from the comparison of the composite and the 29 individual LFs of clusters with $M_{z,\rm lim} \geq -16.5$ mag. Panel **c)**): the z-band DGR distribution of the 29 clusters.

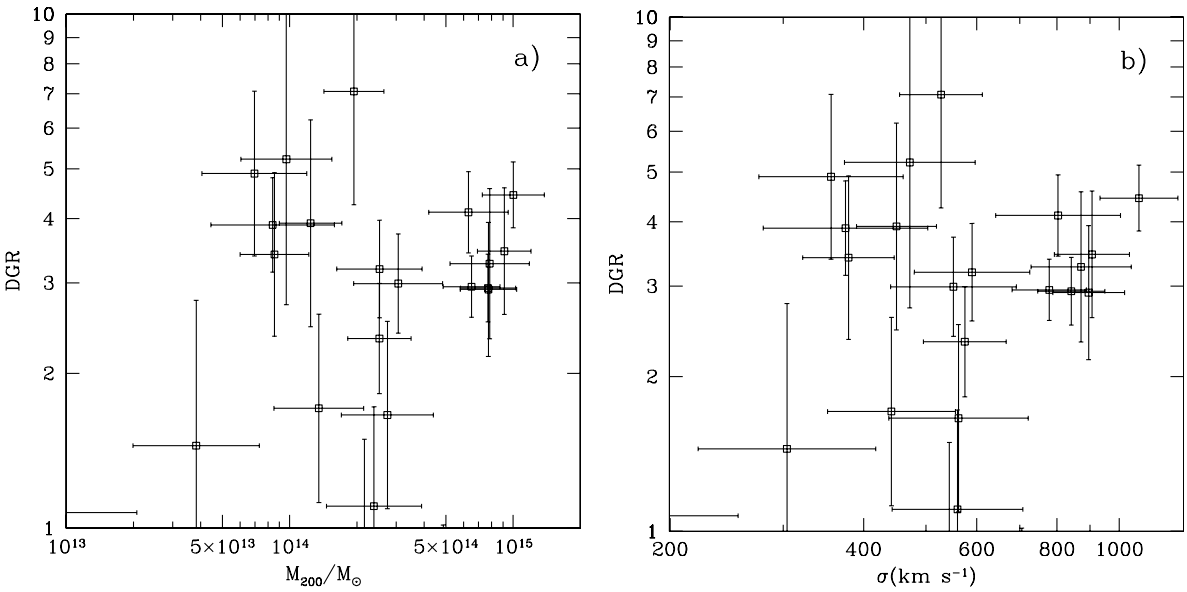

Fig. 6. The z-band DGR within r_{200} as a function of cluster mass (panel **a)**) and the cluster velocity dispersion (panel **b)**). If DGR is calculated within r_{200} the anti-correlation with mass (σ, $L_{\rm X}$ and $L_{\rm op}$) disappears.

($M_{r,\rm lim} \geq -15$). The error bars shown in the figure take into account the galaxy counts Poisson statistics as well as the error due to the background subtraction.

At the redshifts of the 15 clusters considered ($0.02 \leq z \leq 0.05$) early-type galaxies have $u-r$ colors in the range 2.6–2.9 (Fukugita et al. 1995), and galaxies redder than $u-r=3$ are probably in the background. Hence, we can see from Fig. 7a that the residual background contamination after the statistical background subtraction, is generally small (≤10%) and in fact not significant in the bright magnitude range. The contamination is higher for the two clusters RO313 and RX 288, and probably due to the presence of another cluster along the same

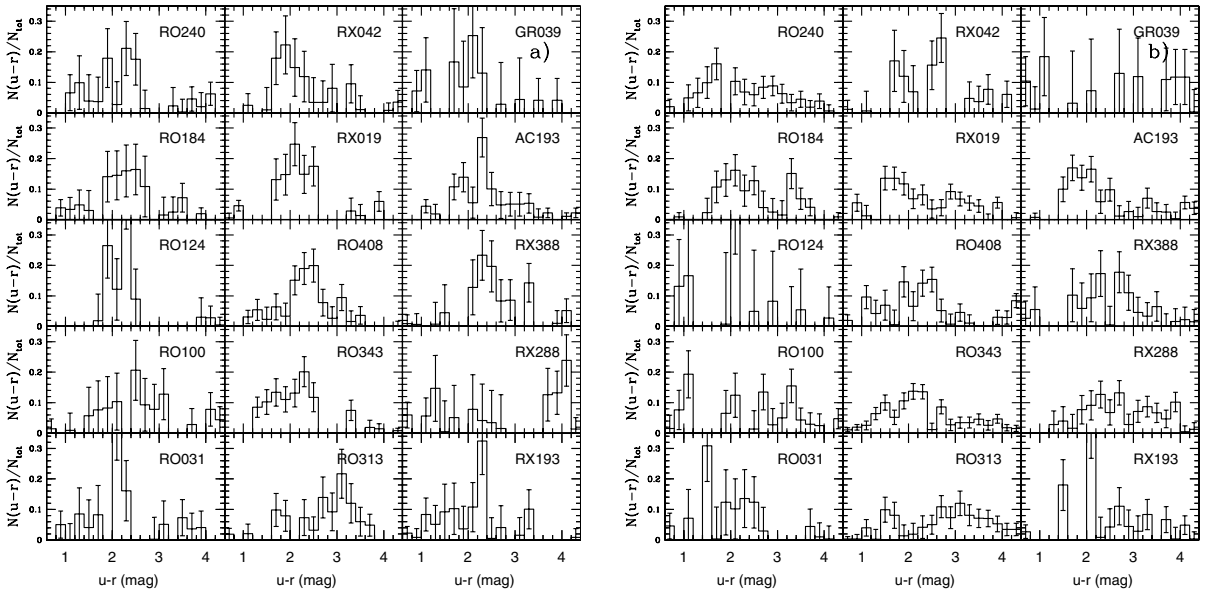

Fig. 7. The background-subtracted $u-r$ distribution of the galaxy members of the 15 clusters with the faintest absolute magnitude limit ($M_{r,\rm lim} \geq -15$). **a)**: Color distribution in the magnitude range $-18 \leq M_r \leq -16.5$; **b)**: color distribution in the magnitude range $-16.5 \leq M_r \leq -15$.

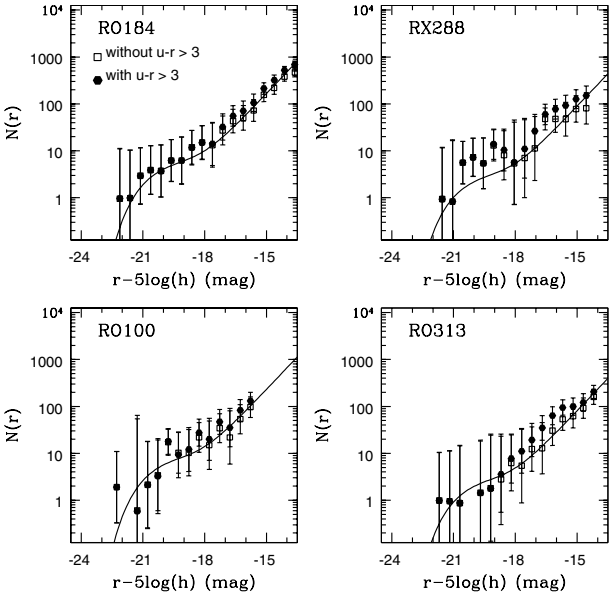

Fig. 8. The LFs of 4 clusters computed as for Fig. 5 (filled points), and by additionally excluding all galaxies with $u-r \geq 3$ (empty squares).

line-of-sight. In the fainter magnitude range, the average background contamination increases to 25–35%, but is still not significant (see Fig. 7b).

If we exclude galaxies with $u-r \geq 3$ from our cluster samples, and recalculate the cluster LFs as before (see Sect. 3), the modifications are marginal (compare filled points and empty squares in Fig. 8). If anything, a better agreement is now found between the composite LF and the individual LF of the cluster R0313, for which the background contamination is more severe, clearly suggesting that the $u-r \geq 3$ color cut helps in cleaning the cluster sample from background contamination.

We therefore adopt the $u-r < 3$ color cut to select cluster members, and, following Strateva et al. (2001) we distinguish between cluster early- and late-type galaxies using a color-cut $u-r = 2.22$. We restrict our analysis to the very nearby clusters ($z \leq 0.1$) to minimize the effects of an uncertain K-correction on the derived colors. The composite LFs of the early- and late-type galaxies (defined on the basis of their $u-r$ colors) are shown in Fig. 9 for four SDSS photometric bands. The late-type galaxy LF is well fitted by a single Schechter function and does not show any evidence of an upturn at the faint end. On the other hand, the early-type LF looks quite different from the late-type LF. It shows a marked bimodal behavior with a pronounced upturn in the faint magnitude region. The best fit parameters are listed in Table 2. Such an upturn is then reflected in the complete (early+late) LF, with the late-type dwarf galaxies contributing to make the faint-end of the complete LF even steeper. This result is in agreement with Yagi et al. (2002). They determine the total LF of 10 clusters within 1 h^{-1} Mpc radius circle. They find that the early-type LF cannot be fitted by a single Schechter function in the magnitude range from −23 to −15, because it flattens at $M_R = -18$ and then rises again.

7. The environmental dependence of the LFs

In order to gain insight into the processes responsible for the shaping of the LF in clusters, we here examine the dependence of the LF on the environmental conditions. In particular we analyze how the LF shape, and the relative fraction of red and blue dwarf galaxies, vary as a function of the clustercentric distance. Figure 10 shows the behavior of the cluster LF calculated within different clustercentric apertures, separately for the early-type (panel a) and late-type (panel b) galaxy populations. Distances are in units of r_{200}. For simplicity we only plot the best fitting functions and not the data-points. The early-type LF is close to a Schechter function at the center of the cluster (within 0.2 r_{200}) and shows a marked upturn afterwards. The location of the upturn varies from -16.2 ± 0.3 mag at distances ≤ 0.3 r_{200} to -17.4 ± 0.4 at distances $\leq r_{200}$.

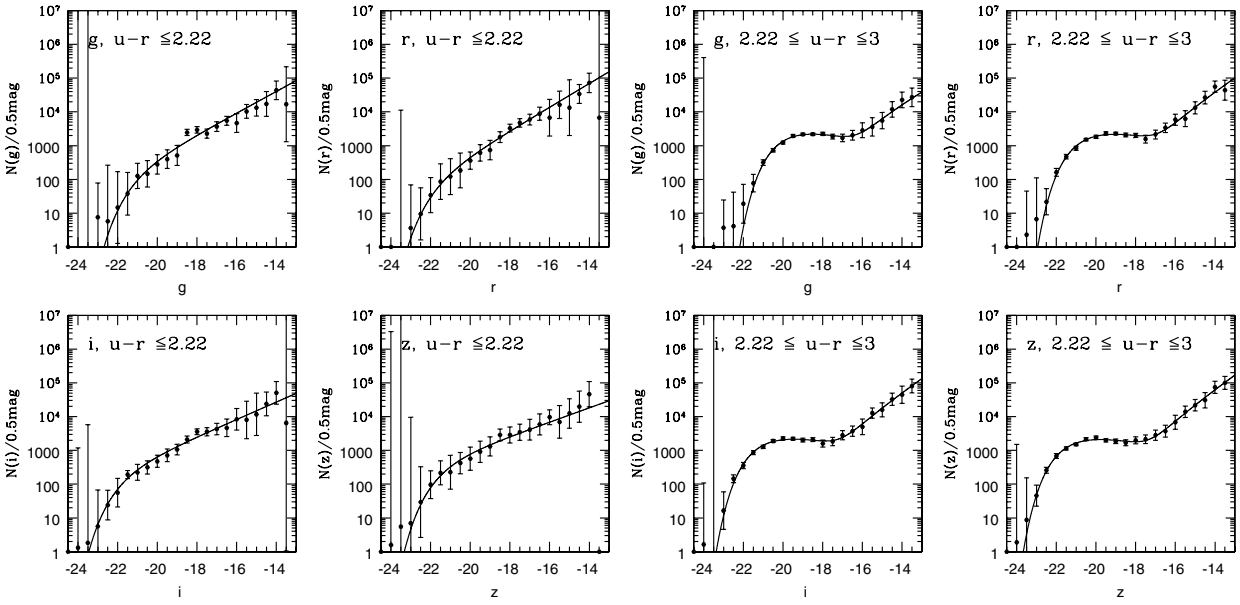

Fig. 9. The composite late-type and early-type LFs in four SDSS photometric bands. The late-type (early-type) LFs are displayed in the four panels on the left (respectively, right).

Table 2. Schechter parameters of the early and late type galaxies composite LFs.

	g	r	i	z
Double Schechter components (r_{200}) for early type galaxies				
α_b	-0.69 ± 0.10	-0.75 ± 0.09	-0.76 ± 0.09	-0.76 ± 0.08
M^*_b	-19.79 ± 0.16	-20.57 ± 0.14	-21.03 ± 0.15	-21.30 ± 0.14
α_f	-1.86 ± 0.15	-2.01 ± 0.11	-2.03 ± 0.08	-2.05 ± 0.09
M^*_f	-17.37 ± 0.21	-18.14 ± 0.15	-18.43 ± 0.15	-18.66 ± 0.14
χ^2/ν	0.72	1.04	1.03	0.90
Single Schechter (r_{200}) for late type galaxies				
α	-1.80 ± 0.04	-1.87 ± 0.04	-1.64 ± 0.02	-1.52 ± 0.05
M^*	-21.13 ± 0.40	-21.71 ± 0.52	-21.79 ± 0.35	-21.52 ± 0.47
χ^2/ν	0.87	0.75	0.90	0.98

The late-type LF is well fitted by a single Schechter function at any clustercentric distance. We do not observe blue galaxies within 0.1 r_{200}. Moreover, the central late-type LF at 0.2 r_{200} is flatter than the LFs in the outer regions and shows a fainter M^*. Since red galaxies are mostly high surface-brightness objects (Blanton et al. 2004), the surface brightness selection effect should be more important for the late-type LF, which, once corrected, would become steeper at the faint-end. If anything, the difference in slope between the faint-ends of the early- and late-type LFs should thus be even larger than observed.

These results are confirmed by the analysis of the early-type LFs in independent clustercentric rings. We consider the region at distances $r \leq 0.3\ r_{200}$ (the central ring), $0.3 \leq r/r_{200} \leq 0.7$ (the intermediate ring) and $0.7 \leq r/r_{200} \leq 1$ (the outer ring). The best fitting functions of the cluster early-type LFs within these regions are shown in Fig. 11. In order to emphasize the *shape* variation of the LF, all three LFs are renormalized to the same value. The upturn at the faint end is brighter in the outer ring than in the central one, confirming the previous analysis. Moreover, the shape of the bright end of the cluster LF seems to be absolutely independent from the faint end. The values of M^* and the slope of the bright end are consistent within the errors in the three regions (as found in Paper II). This suggests that the process of formation of the bright cluster galaxies (with magnitude brighter that $M^* - 2$ mag) is the same in all the cluster environments. Therefore, it seems unlikely that the lack of dwarf systems observed at the center of the cluster is due to a hierarchical process of formation of the bright central galaxies. Indeed, in that case we should observe also a lack of bright galaxies in the outer ring in favor of large amount of dwarf systems, which is not observed.

The analysis so far provides only results about the LF *shape*. In order to quantify the relative contribution of the early- and late-type dwarf galaxy populations to the faint end of the LF, and its dependence on the environment, we analyse the radial (cumulative and differential) profile of the dwarf systems in the clusters. For this, we consider the galaxies with $-18 \leq M_r \leq -15$, and to improve the statistics, we stack the clusters with $M_{r,\rm lim} \geq -15$ mag, by rescaling the clustercentric distances in units of r_{200}. The cumulative profiles of the fractions of dwarf galaxies of both the early- and the late-type are shown in Fig. 12a. The center ($\leq 0.4\ r_{200}$) contains less than 30% of dwarf galaxies (half of them are red systems), in the selected magnitude range. Dwarf galaxies are more

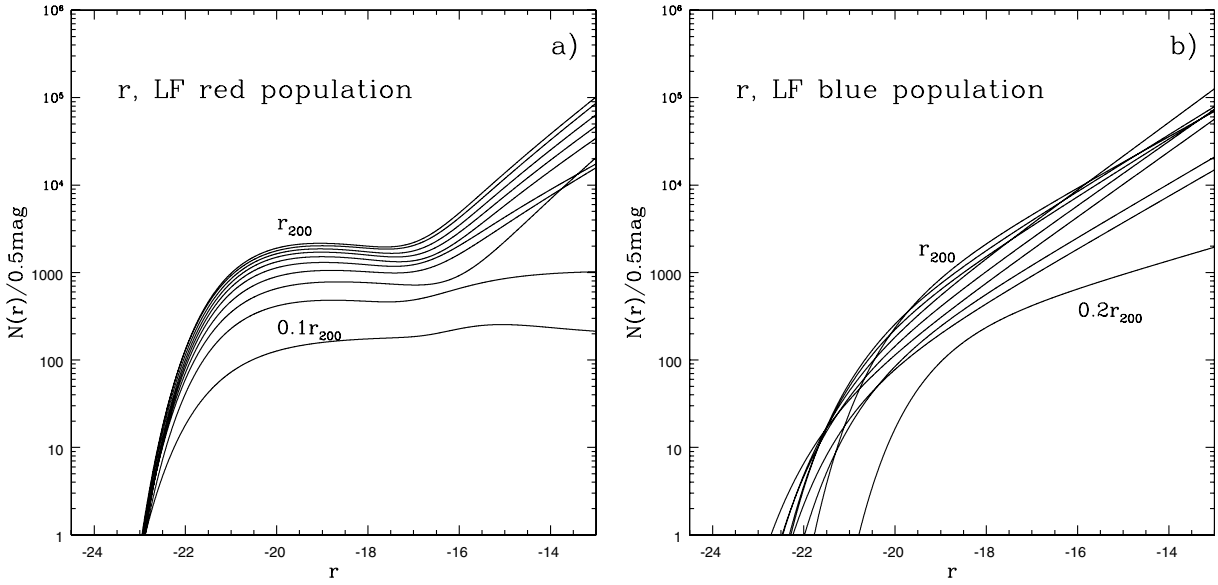

Fig. 10. The cluster LFs within different cluster apertures in the r band per morphological type. The increment of the apertures is $0.1 \times r_{200}$. The normalization of the fitting function is increasing at larger apertures. Panel **a)** shows the LF of the cluster red galaxy population, calculated within different clustercentric apertures expressed in unit of r_{200}. Panel **b)** shows the same for the cluster blue galaxy population. For simplicity we only plot the best fitting functions and not the data points.

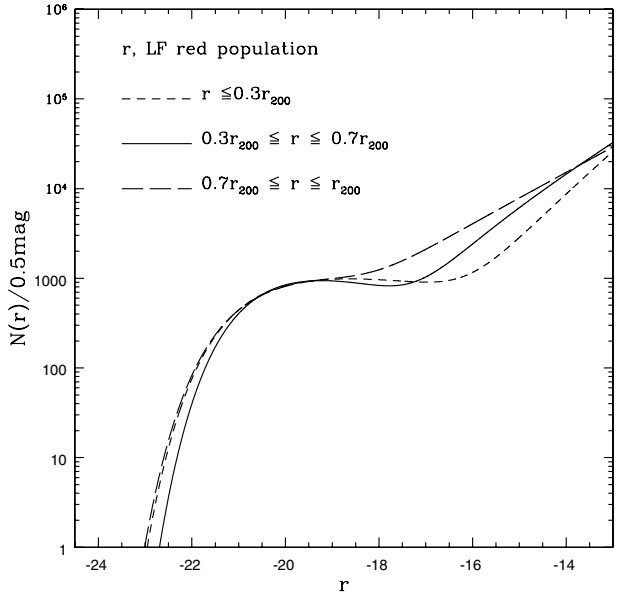

Fig. 11. The early-type LF calculated within three different cluster regions. Only the best fitting functions are plotted, for simplicity, and not the data points. The LFs are renormalized to the same value to emphasize the shape variations.

abundant in the cluster outskirts; the high-density environment in the cluster cores is hostile to dwarf galaxies. This phenomenology has already been observed in several individual clusters (see e.g. Lobo et al. 1997; Boyce et al. 2001; Mercurio et al. 2003; Dahlen et al. 2004).

The early-type dwarf galaxies represents 35% of the whole dwarf population within r_{200}, i.e. most of the dwarf galaxies are of late-type. However, the dwarf early-type galaxies are the dominant dwarf population region within 0.4 r_{200}, their relative fraction reaching a plateau at ≃0.6 r_{200}, while the late-type dwarf galaxies are more abundant in clusters outskirts. This is confirmed also by the ratio between early- and late-type dwarf galaxies calculated in contiguous clustercentric rings (differential profile, see Fig. 12b). The number of early-type dwarf galaxies is twice the number of late-type dwarf galaxies within 0.2 r_{200} and then decreases to 1/2 at larger distances.

The relation between dwarf morphology and clustercentric distance translates into a morphology-density relation. In Fig. 12d we show the ratio between early- and late-type dwarf galaxies as a function of the number density of galaxies brighter than $M_r \leq -18$ (the bright galaxies number density profile is shown in panel c of the same figure). As expected, the early-type dwarf galaxies dominate in high density regions, while the late-type dwarf galaxies are frequent in low density regions. Clearly, the well known morphology density relation for cluster galaxies (Dressler 1980) has an extension into the dwarf regime.

7.1. Comparison with the field

In order to extend the morphology-density relation for dwarf cluster galaxies outside clusters, we extract a subsample of galaxies from the SDSS spectroscopic sample. We select a fairly complete sample of galaxies in the redshift range $z \leq 0.02$ and in the magnitude range $-18 \leq M_r \leq -16$. The late-type galaxies ($u - r \leq 2.22$) represent the 93% of the galactic population in that range of magnitude, in agreement with the results of Blanton et al. (2004). We then calculate for each galaxy in the sample the local density of galaxy neighbors, by counting the number of systems with $M_r \leq -18$ mag, within 2.5 Mpc projected radius and ± 500 km s^{-1} of the galaxy position and redshift. We divide the subsample in late and early-type galaxies using the color cut of Strateva et al. (2001). Figure 13 shows the number of galaxies per bin of local density for the two

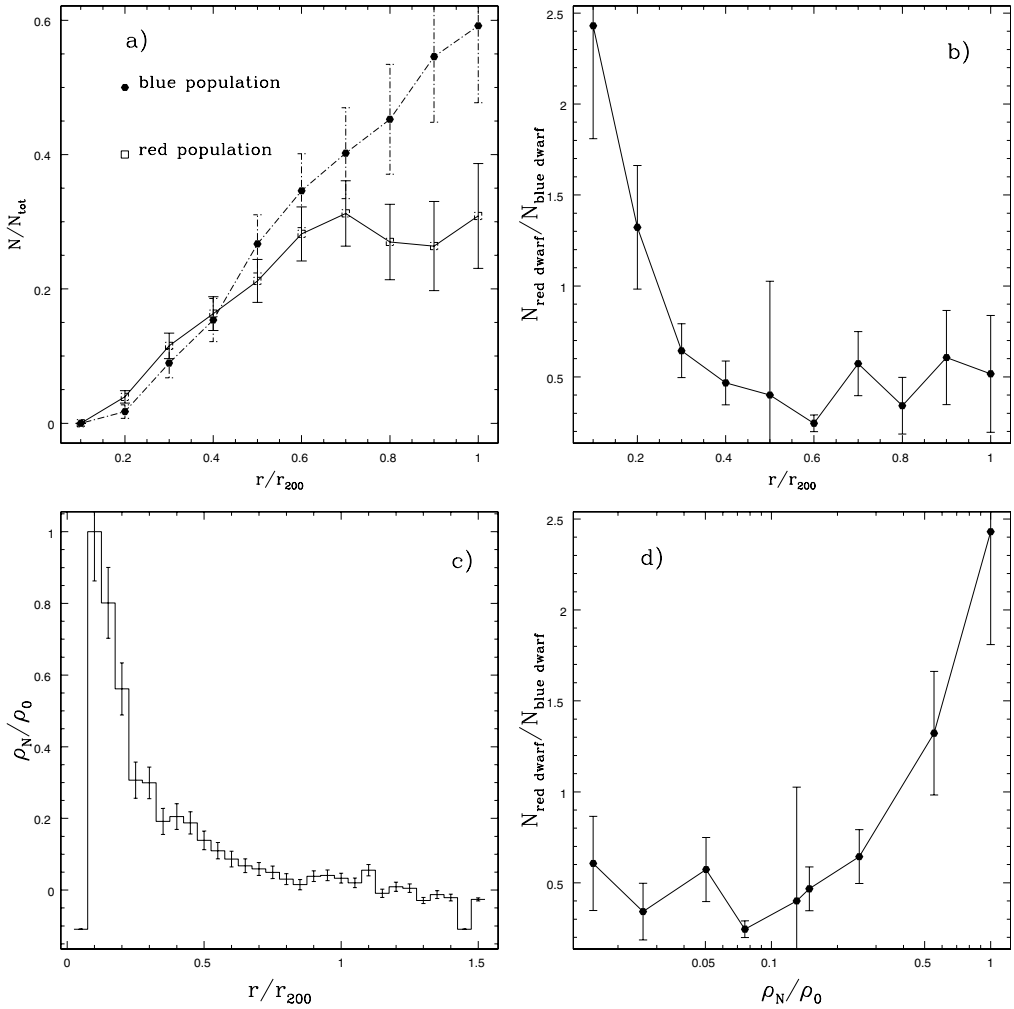

Fig. 12. The fraction of red and blue dwarf galaxies as a function of the cluster environments. Panel **a)** shows the cumulative radial profile of the fraction of blue (filled points) and red (empty squared) dwarf galaxies ($-18 \leq M_r \leq -15$ mag). The fraction is defined on the total number of cluster dwarf galaxies in the considered magnitude range. Panel **b)** shows the differential radial profile of the ratio between red and blue dwarf galaxies. Panel **c)** shows the differential radial profile of the surface density of the bright cluster galaxies in clusters ($M_r \leq -18$ mag). Panel **d)** shows the relation between the surface density of bright galaxies and the fraction of red and blue dwarf galaxies calculated in the same clustercentric ring.

galaxy types. It is clear that late-type galaxies (dashed dotted histogram) populate the very low density regions, while the early-type galaxies distribution (solid histogram) has a much larger spread, with 50% of the systems located in regions with more than 10 galaxy neighbors.

It is also interesting to compare our composite cluster LFs with the LF of field galaxies. Blanton et al. (2005) have recently derived the LF of field SDSS galaxies down to −12 mag. Their LF have a very weak upturn, much shallower and at a fainter carachteristic magnitude than in our cluster LF. The faint-end slope of their LF is −1.3, but could be steeper (−1.5) if a correction is applied to account for low surface-brightness selection effects. The LF of *blue* field galaxies is even steeper, but the authors do not report the value of the faint-end slope. A similar faint-end slope (−1.5) has also been found by Madgwick et al. (2002) for the LF of field galaxies from the 2dF survey. They also noticed an upturn in the LF, due to an overabundance of early-type galaxies, making it impossible to fit the LF adequately with a single Schechter function. A previous determination of the SDSS field LF was obtained by Nakamura et al. (2003). They found a slope of ∼−1.9 for dIrr, consistent with the value found by Marzke et al. (1994) for the CfA survey.

The faint-end slope of our late-type cluster galaxies LF is steeper than most field LFs for the same galaxy type (see Table 3 in Paper II) but consistent with those of Nakamura et al. (2003) and Marzke et al. (1994). Given the large variance of results for the field LFs, possibly due to the different magnitude limits adopted, or to poor statistics in the fainter bins of the LF (see de Lapparent 2003 for a thorough discussion on this topic), we conclude there is no significant difference between the late-type LF in clusters and the field.

8. Discussion

There are many observations and theoretical models in the literature (see, e.g., De Propris et al. 2003) that try to explain the formation and evolution of cluster galaxies, red dwarf galaxies in particular. According to the hierarchical picture for structure

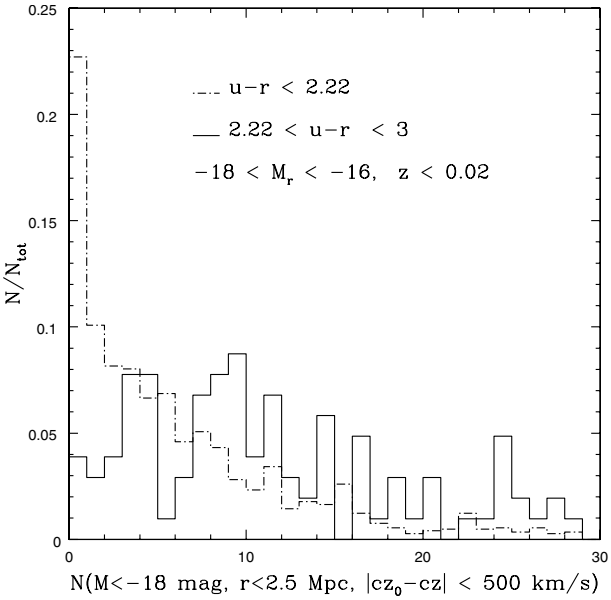

Fig. 13. The density distribution of neighbors of late (dotted histogram) and early (solid histogram) galaxies in the field. We select a fairly complete sample of nearby galaxies ($z \leq 0.02$) from the Sloan spectroscopic sample in the magnitude region $-18 \leq M_R \leq -16$. We calculate for each galaxy in the sample the local density of neighbor galaxies counting the number of systems with $M_R \leq -18$ mag, within 2.5 Mpc projected radius and ± 500 km s^{-1} of the galaxy position and redshift. The sample comprises 1561 systems.

formation, small dark matter haloes form before large ones. If one identifies the dwarf galaxies with the small dark matter haloes, they are predicted to origin soon after the structure formation began. Dwarf ellipticals would then be old, passively evolved galaxies. This scenario seems to be inconsistent with the observations of a large spread in age and metallicity in the clusters dwarf early-type galaxies (Conselice et al. 2001, 2003; Rakos et al. 2001). Hence, dwarf ellipticals must have had a delayed star formation epoch. The delay could be originated by the intense ultraviolet background intensity at high redshift, keeping the gas of the dwarf galaxies photoionized until $z \sim 1$, or, perhaps by the intra-cluster medium confinement. The intra-cluster medium pressure could avoid dwarf galaxies losing their gas content by SN ejecta. However, this possibility would require a much more centrally concentrated distribution of dwarf ellipticals in clusters than is observed.

In alternative, the excess of dwarf early-type galaxies in clusters could origin from the evolution of field dIrr when they are accreted by the clusters. The evolution of dIrr into dwarf early-type galaxies is supported by the result of van Zee et al. (2004), namely that there is significant similarity in the scaling relations and properties of dIrr and dEs. A scenario where *all* dwarf early-type galaxies evolve from dIrr via disk fading does not however seem possible, because many dEs in the Virgo and Fornax clusters are brighter than the dIrr (Conselice et al. 2001).

Perhaps, some dwarf early-type galaxies evolve from dIrr and some evolve from spirals. The evolution of spirals into dwarf spheroidals can occur via the process of "galaxy harassment" proposed by Moore et al. (1996, 1998). In this scenario, close, rapid encounters between galaxies can lead to a radical transformation of a galaxy morphology. Gas and stars are progressively stripped out of the disk systems, eventually leaving a spheroidal remnant, that resembles an S0 galaxy or a dwarf spheroidal, depending on the size of the progenitor. Direct support for the harassment scenario comes from the discoveries of disks or even spiral arms in dwarf early-type cluster galaxies (Jerjen et al. 2000; Barazza et al. 2002; Graham et al. 2003). Indirect support comes from the similar velocity distribution of dwarf cluster galaxies (Drinkwater et al. 2001) and gas-rich spirals and irregulars (Biviano et al. 1997), both suggesting infalling orbits.

Is the harassment scenario still viable in view of our results? We can draw the following conclusions from our observational results. First, the universality of the cluster LF suggests that whatever shapes the cluster LF is not strictly dependent on the cluster properties. Second, the difference between the cluster and field LF seems to be related to an excess of dwarf early-type galaxies in clusters. Hence, there is a cluster-related process that leads to the formation of dwarf early-type galaxies, regardless of the cluster intrinsic properties. The process cannot be related, e.g., to the intra-cluster gas density, or the cluster velocity dispersion, or the cluster mass, hence, a process like ram-pressure would seem to be ruled out.

The density dependence of the relative number of early- and late-type dwarfs suggests that the shaping of the cluster LF is related to the excess mean density relative to the field, which is the same for all clusters if, as we have done, the cluster regions are defined within a fixed overdensity radius (r_{200} in our case). In other words, the transformation of spirals, and perhaps, dIrr, into dwarf spheroidals or dEs, seems to be a threshold process that occurs when the local density exceeds a given threshold. Judging from Fig. 12, this threshold seems to occur at a clustercentric distance of $\sim$0.6–0.7 r_{200}.

We have also found that the relative number of dwarf early- and late-type galaxies increases with decreasing clustercentric distance (and increasing density). Galaxies near the cluster center are probably an older cluster population, accreted when the cluster was smaller, according to the hierarchical picture of cluster formation and evolution. Hence, these centrally located galaxies have had more time to accomplish the morphology transformation than galaxies located in the cluster outskirts, which are more recent arrivals.

On the other hand, very near the cluster center, an additional process must be at work to explain our observed fading of the upturn of the cluster early-type LF, and the decrease of both the early- and the late-type dwarf-to-giant galaxy ratio with decreasing clustercentric distance. High-velocity dispersions in clusters inhibit merging processes (e.g. Mihos 2004), hence it is unlikely that dwarf galaxies merge to produce bigger galaxies at the cluster centers. Consistently, we find that the shape of the bright-end of the early-type LF does not depend on the environment, which suggests that bright early-type galaxies are not a recent product of the cluster environment. In fact, the luminosity density profile of bright early-type galaxies has not evolved significantly since redshift $z \sim 0.5$ (Ellingson 2003).

The most likely explanation for the lack of dwarf galaxies near the cluster center is tidal or collisional disruption of the

dwarf galaxies. The fate of the disrupted dwarfs is probably to contribute to the intra-cluster diffuse light (e.g. Feldmeier et al. 2004; Murante et al. 2004; Willman et al. 2004).

The difference between the cluster and field LF could thus be explained as a difference in morphological mix, plus a density-dependent dwarf early-type galaxies LF, that, added to an invariant bright early-type LF, produces a more or less important and bright upturn, depending on the density of the environment.

9. Conclusion

We have presented a detailed analysis of the cluster individual and composite luminosity functions down to -14 mag in all the Sloan photometric bands. All the luminosity functions are calculated within the physical size of the systems given by r_{500} and r_{200}. The main conclusions of our analysis are as follows:

- We confirm that the composite LF shows a bimodal behavior with a marked upturn at the faint magnitude range. A double Schechter component function is the best fit for the cluster LF. We show that calculating the individual and the composite LF within a fixed aperture for all the systems introduces selection effects. These selection effects justify the differences observed in the faint end of the individual cluster LFs studied in Paper II and the anti-correlations between DGR and the global cluster properties (mass, velocity dispersion, optical and X-ray luminosities) observed in this work. If the cluster LF is calculated within the physical size of the system (r_{500} or r_{200}), the differences due to aperture effects disappear and the individual cluster LF is well represented by the composite LF. Therefore, we conclude that the shape of the cluster LF is universal in all the magnitude ranges.
- We use the $u - r$ color to study the color distribution of the faint cluster galaxies. The color distribution confirms that the contamination due to background galaxies is due to field-to-field variance of the background. We apply the color cut at $u - r = 2.22$ suggested by Strateva et al. (2001) to separate early-type from late-type galaxies and study the composite LF by morphological type. We observe that the upturn at the faint magnitudes shown by the complete LF is due to early-type galaxies while the late-type LF is well represented by a single Schechter function.
- We study the cumulative and the differential radial profile of the faint early- and late-type galaxies in clusters. The faint early-type galaxies are concentrated in the central regions while the faint late-type galaxies dominate the outskirts of the systems. The analysis of the color-density relation in a reference sample of nearby galaxies selected from the SDSS spectroscopic sample suggests that red galaxies could be a typical cluster galaxy population. Our analysis show that the bright red population seems to have a luminosity distribution absolutely independent from the behavior of the faint red galaxies in different environments. We observe a fading of the LF upturn toward the cluster core.
- We propose to interpret our results in term of a combination of two processes, transformation of spirals and dIrr into dwarf early-type galaxies via harassment, and disruption of dwarf galaxies near the cluster center by collisions and/or tidal effects.

Whether galaxies evolve from one type to another, in response to the local density, to create the morphology-density relation, or whether the relation is established when the galaxies form, is still an open issue (see, e.g., Dressler 2004). Photometric data alone cannot provide conclusive indications about the nature and the origin of the dwarf population in cluster. In this respect, it would be very useful to sample the velocity distributions of a large set of dwarf galaxies in clusters, in order to constrain their orbital characteristics as it has recently been done for bright cluster galaxies (Biviano & Katgert 2004). If the dwarf early-type galaxies evolve from spirals, radially elongated orbits are expected, while if dwarf early-type galaxies are a more pristine cluster population, their orbits should resemble the isotropic orbits of ellipticals. Additional insights may come from higher accuracy spectroscopy of the dwarf galaxies, allowing to deduce information about their internal velocity dispersion and metallicity, which could be used to put constraints on their age (see, e.g., Kauffmann et al. 2004; Carretero et al. 2004).

Acknowledgements. We would like to thank Gwenael Boué and the anonymous referee for the usefull comments which significantly improved the paper.
Funding for the creation and distribution of the SDSS Archive has been provided by the Alfred P. Sloan Foundation, the Participating Institutions, the National Aeronautics and Space Administration, the National Science Foundation, the US Department of Energy, the Japanese Monbukagakusho, and the Max Planck Society. The SDSS Web site is `http://www.sdss.org/`. The SDSS is managed by the Astrophysical Research Consortium (ARC) for the Participating Institutions. The Participating Institutions are The University of Chicago, Fermilab, the Institute for Advanced Study, the Japan Participation Group, The Johns Hopkins University, Los Alamos National Laboratory, the Max-Planck-Institute for Astronomy (MPIA), the Max-Planck-Institute for Astrophysics (MPA), New Mexico State University, University of Pittsburgh, Princeton University, the United States Naval Observatory, and the University of Washington.

References

Abazajian, K., Adelman-McCarthy, J., Agüeros, M., et al. 2003, AJ, 126, 2081
Andreon, S. 2004, A&A, 416, 865
Barazza, F. D., Binggeli, B., & Jerjen, H. 2002, A&A, 391, 823
Beers, T. C., Flynn, K., & Gebhardt, K. 1990, AJ, 100, 32
Beijersbergen, M., Hoekstra, H., van Dokkum, P. G., & van der Hulst, T. 2002, MNRAS, 329, 385
Biviano, A., & Girardi, M. 2003, ApJ, 585, 205
Biviano, A., & Katgert, P. 2004, A&A, 424, 779
Biviano, A., Durret, F., Gerbal, D., et al. 1995, A&A, 297, 610
Biviano, A., Katgert, P., Mazure, A., et al. 1997, A&A, 321, 84
Blanton, M. R., Lin, H., Lupton, R. H., et al. 2003, AJ, 125, 2276
Blanton, M. R., Lupton, R. H., Schlegel, D. J., et al. 2005, ApJ, 631, 208
Böhringer, H., Voges, W., Huchra, J. P., et al. 2000, ApJS, 129, 435
Böhringer, H., Collins, C. A., Guzzo, L., et al. 2002, ApJ, 566, 93
Boyce, P. J., Phillips, S., Jones, J. B., et al. 2001, MNRAS, 328, 277

Carretero, C., Vazdekis, A., Beckman, J. E., Sánchez-Blázquez, P., & Gorgas, J. 2004, ApJ, 609, L45
Christlein, D., & Zabludoff, A. 2003, ApJ, 591, 764
Cole, S., Aragon-Salamanca, A., Frenk, C. S., Navarro, J. F., & Zepf, S. E. 1994, MNRAS, 271, 781
Colless, M. 1989, MNRAS, 237, 799
Conselice, C. J., Gallagher, J. S. III, & Wyse, R. F. G. 2001, ApJ, 559, 791
Conselice, C. J., Gallagher, J. S. III, & Wyse, R. F. G. 2003, AJ, 125, 66
Cortese, L., Gavazzi, G., Boselli, A., et al. 2003, A&A, 410, L25
Cross, N. J. G., Driver, S. P., Liske, J., et al. 2004, MNRAS, 349, 576
Dahlén, T., Fransson, C., Östlin, G., & Näslund, M. 2004, MNRAS, 350, 253
Davies, J. I., Roberts, S., & Sabatini, S. 2005, MNRAS, 356, 794
de Lapparent, V. 2003, A&A, 408, 845
De Propris, R., Colless, M., Driver, S. P., et al. 2003, MNRAS, 342, 725
De Propris, R., Pritchet, C. J., Harris, W. E., & McClure, R. D. 1995, ApJ, 450, 534
Dolag, K., Bartelmann, M., Perrotta, F., et al. 2004, A&A, 416, 853
Dressler, A. 1978, ApJ, 223, 765
Dressler, A. 1980, ApJ, 236, 351
Dressler, A. 2004, in Clusters of Galaxies: Probes of Cosmological Structure and Galaxy Evolution ed. J. S. Mulchaey, A. Dressler, & A. Oemler Jr. (Cambridge University Press), 206
Drinkwater, M. J., Gregg, M. D., & Colless, M. 2001, ApJ, 548, L139
Driver, S. P., Phillips, S., Davies, J. I., Morgan, I., & Disney, M. J. 1994, MNRAS, 268, 393
Durret, F., Slezak, E., Lieu, R., Dos Santos, S., & Bonamente, M. 2002, A&A, 390, 397
Eisenstein, D. J., Annis, J., Gunn, J. E., et al. 2001, AJ, 122, 2267
Ellingson, E. 2003, Ap&SS, 285, 9
Feldmeier, J. J., Ciardullo, R., Jacoby, G. H., & Durrell, P. R. 2004, ApJ, 615, 196
Fukugita, M., Shimasaku, K., & Ichikawa, T. 1995, PASP, 107, 945
Fukugita, M., Ichikawa, T., Gunn, J. E., et al. 1996, AJ, 111, 1748
Garilli, B., Maccagni, D., & Andreon, S. 1999, A&A, 342, 408
Girardi, M., Biviano, A., Giuricin, G., Mardirossian, F., & Mezzetti, M. 1993, ApJ, 404, 38
Girardi, M., Giuricin, G., Mardirossian, F., Mezzetti, M., & Boschin, W. 1998, ApJ, 505, 74
Goto, T., Sekiguchi, M., Nichol, R. C., et al. 2002, AJ, 123, 1807
Graham, A. W., Jerjen, H., & Guzmán, R. 2003, AJ, 126, 1787
Gunn, J. E., & Gott, J. R. III 1972, ApJ, 176, 1
Gunn, J. E., Carr, M., Rockosi, C., et al. 1998, AJ, 116, 3040
Hilker, M., Mieske, S., & Infante, L. 2003, A&A, 397, L9
Hogg, D. W., Finkbeiner, D. P., Schlegel, D. J., & Gunn, J. E. 2001, AJ, 122, 2129
Horner, D. 2001, Ph.D. Thesis, University of Maryland
Jerjen, H., Kalnajs, A., & Binggeli, B. 2000, A&A, 358, 845
Katgert, P., Biviano, A., & Mazure, A. 2004, ApJ, 600, 657
Kauffmann, G., White, S. D. M., & Guiderdoni, B. 1993, MNRAS, 264, 201
Kauffmann, G., White, S. D. M., Heckman, T. M., et al. 2004, MNRAS, 353, 713
Liske, J., Lemon, D. J., Driver, S. P., et al. 2003, MNRAS, 344, 307
Lobo, C., Biviano, A., Durret, F., et al. 1997, A&A, 317, 385
Loveday, J. 1997, ApJ, 489, 29
Lugger, P. M. 1986, ApJ, 303, 535
Lugger, P. M. 1989, ApJ, 343, 572
Lumsden, S. L., Collins, C. A., Nichol, R. C., Eke, V. R., & Guzzo, L. 1997, MNRAS, 290, 119
Lupton, R. H., Gunn, J. E., & Szalay, A. S. 1999, AJ, 118, 1406
Madgwick, D. S., Lahav, O., Baldry, I. K., et al. 2002, MNRAS, 333, 133
Marzke, R. O., Geller, M. J., Huchra, J. P., & Corwin, H. G. Jr. 1994, AJ, 108, 437
Menci, N., Cavaliere, A., Fontana, A., Giallongo, E., & Poli, F. 2002, ApJ, 575, 18
Mercurio, A., Massarotti, M., Merluzzi, P., et al. 2003, A&A, 408, 57
Mihos, J. C. 2004, in Clusters of Galaxies: Probes of Cosmological Structure and Galaxy Evolution ed. J. S. Mulchaey, A. Dressler, & A. Oemler Jr. (Cambridge University Press), 277
Mobasher, B., Colless, M., Carter, D., et al. 2003, ApJ, 587, 605
Moore, B., Katz, N., Lake, G., Dressler, A., & Oemler, A. Jr. 1996, Nature, 379, 613
Moore, B., Lake, G., & Katz, N. 1998, ApJ, 495, 139
Mulchaey, J. S., Davis, D. S., Mushotzky, R. F., & Burstein, D. 2003, ApJS, 145, 39
Murante, G., Arnaboldi, M., Gerhard, O., et al. 2004, ApJ, 607, L83
Nakamura, O., Fukugita, M., Yasuda, N., et al. 2003, AJ, 125, 1682
Navarro, J. F., Frenk, C. S., & White, S. D. M. 1996, ApJ, 462, 563
Navarro, J. F., Frenk, C. S., & White, S. D. M. 1997, ApJ, 490, 493
Paolillo, M., Andreon, S., Longo, G., et al. 2001, A&A, 367, 59
Phillips, S., & Driver, S. 1995, MNRAS, 274, 832
Phillips, S., Driver, S. P., Couch, W. J., & Smith, R. M. 1998, ApJ, 498, L119
Popesso, P., Böhringer, H., Brinkmann J., Voges, W., & York, D. G. 2004b, A&A, 423, 449 (Paper I)
Popesso, P., Böhringer, H., Romaniello, M., & Voges, W. 2004a, A&A, accepted [arXiv:astro-ph/0410011] (Paper II)
Popesso, P., Biviano, A., Böhringer, Romaniello, M., & Voges, W. 2004c, A&A, accepted [arXiv:astro-ph/0411536] (Paper III)
Pracy, M. B., De Propris, R., Driver, S. P., Couch, W. J., & Nulsen, P. E. J. 2004, MNRAS, 352, 1135
Rakos, K., Schombert, J., Maitzen, H. M., Prugovecki, S., & Odell, A. 2001, AJ, 121, 1974
Rauzy, S., Adami, C., & Mazure, A. 1998, A&A, 337, 31
Retzlaff, J. 2001, in Clusters of galaxies and the high redshift universe in X-rays. Recent results of XMM-Newtomn and Chandra, XXIst Moriond Astrophysics Meeting, March 10–17, 2001 Savoie, France, ed. D. M. Neumann, & J. T. T. Van
Sabatini, S., Davies, J., Scaramella, R., et al. 2003, MNRAS, 341, 981
Schechter, P. 1976, ApJ, 203, 297
Schlegel, D., Finkbeiner, D. P., & Davis, M. 1998, ApJ, 500, 525
Smith, R. M., Driver, S. P., & Phillips, S. 1997, MNRAS, 287, 415
Smith, J. A., Tucker, D. L., Kent, S., et al. 2002, AJ, 123, 2121
Stoughton, C., Lupton, R. H., Bernardi, M., et al. 2002, AJ, 123, 485
Strateva, I., Ivezić, Z., Knapp, G., et al. 2001 AJ, 122, 1861
Strauss, M. A., Weinberg, D. H., Lupton, R. H., et al. 2002, AJ, 124, 1810
The, L. S., & White, S. D .M. 1986, AJ, 92, 1248
Thompson, L. A., & Gregory, S. A. 1993, AJ, 106, 2197
Trentham, N. 1998, MNRAS, 295, 360
Trentham, N., Tully, R. B., & Verheijen, M. A. W. 2001, MNRAS, 325, 385
Tully, R. B., Somerville, R. S., Trentham, N., & Verheijen, M. A. 2002, ApJ, 569, 573
Ulmer, M. P., Bernstein, G. M., Martin, D. R., et al. 1996, AJ, 112, 2517
Valotto, C., Nicotra, M. A., Muriel, H., & Lambas, D. G. 1997, ApJ, 479, 90
van Zee, L., Skillman, E. D., & Haynes, M. P. 2004, AJ, 128, 121
Willman, B., Governato, F., Wadsley, J., & Quinn, T. 2004, MNRAS, 355, 159
Yagi, M., Kashikawa, N., Sekiguchi, M., et al. 2002, AJ, 123, 87
York, D. G., Adelman, J., Anderson, J. E. Jr., et al. 2000, AJ, 120, 1579